mRNA spindle localization and mitotic translational regulation by CPEB1 and CPEB4

ROSA PASCUAL,[1,6] CAROLINA SEGURA-MORALES,[1,7] MANJA OMERZU,[2] NICOLÁS BELLORA,[3] EULÀLIA BELLOC,[1] CHIARA LARA CASTELLAZZI,[1] OSCAR REINA,[1] EDUARDO EYRAS,[4,5,8] MADELON M. MAURICE,[2] ALBA MILLANES-ROMERO,[1] and RAÚL MÉNDEZ[1,5]

[1]Institute for Research in Biomedicine (IRB Barcelona), The Barcelona Institute of Science and Technology, 08028 Barcelona, Spain

[2]Oncode Institute and Department of Cell Biology, Centre for Molecular Medicine, University Medical Centre Utrecht, 3584 CX Utrecht, The Netherlands

[3]Instituto Andino Patagónico de Tecnologías Biológicas y Geoambientales (IPATEC), Universidad Nacional del Comahue—CONICET, S.C. de Bariloche, 8400, Argentina

[4]Department of Experimental and Health Sciences, Universidad Pompeu Fabra, Barcelona 08002, Spain

[5]Institució Catalana de Recerca i Estudis Avançats (ICREA), Barcelona 08010, Spain

ABSTRACT

Transition through cell cycle phases requires temporal and spatial regulation of gene expression to ensure accurate chromosome duplication and segregation. This regulation involves dynamic reprogramming of gene expression at multiple transcriptional and posttranscriptional levels. In transcriptionally silent oocytes, the CPEB-family of RNA-binding proteins coordinates temporal and spatial translation regulation of stored maternal mRNAs to drive meiotic progression. CPEB1 mediates mRNA localization to the meiotic spindle, which is required to ensure proper chromosome segregation. Temporal translational regulation also takes place in mitosis, where a large repertoire of transcripts is activated or repressed in specific cell cycle phases. However, whether control of localized translation at the spindle is required for mitosis is unclear, as mitotic and acentriolar-meiotic spindles are functionally and structurally different. Furthermore, the large differences in scale-ratio between cell volume and spindle size in oocytes compared to somatic mitotic cells may generate distinct requirements for gene expression compartmentalization in meiosis and mitosis. Here we show that mitotic spindles contain CPE-localized mRNAs and translating ribosomes. Moreover, CPEB1 and CPEB4 localize in the spindles and they may function sequentially in promoting mitotic stage transitions and correct chromosome segregation. Thus, CPEB1 and CPEB4 bind to specific spindle-associated transcripts controlling the expression and/or localization of their encoded factors that, respectively, drive metaphase and anaphase/cytokinesis.

Keywords: mRNA localization; mRNA translation; mitosis; spindle; CPEB

INTRODUCTION

In the transcriptionally dormant stages of early development, gene expression relies on the spatial and temporal regulation of maternal mRNAs translation. This reprogramming is needed to complete meiosis and for the first embryonic mitotic divisions. The main mechanisms directing the translational repression and later reactivation of maternal mRNAs during meiosis are, respectively, the shortening and then elongation of their poly(A) tails. This cytoplasmic polyadenylation requires the cytoplasmic polyadenylation element (CPE), which is present in the 3′-UTRs of the maternal mRNAs and is bound by the CPE-binding protein (CPEB) family of RNA-binding proteins (Richter 2007; Weill et al. 2012). In meiosis, the specific combination of CPEs define the timing and extent of the activation and the localization of the mRNA (Belloc and Mendez 2008; Eliscovich et al. 2008; Pique et al. 2008). The sequential activation of the CPE-regulated mRNAs is also ensured by phase

[6]**Present address:** Cancer Biology and Stem Cells Division, The Walter and Eliza Hall Institute of Medical Research, Parkville, Victoria 3052 Australia

[7]**Present address:** Centre for Genomic Regulation (CRG), UPF, 08003, Barcelona, Spain

[8]**Present address:** The John Curtin School of Medical Research, Australian National University, Canberra, Acton, 2601, Australia

Corresponding authors: raul.mendez@irbbarcelona.org, alba.millanes@irbbarcelona.org

Article is online at http://www.rnajournal.org/cgi/doi/10.1261/rna.077552.120.

specific functions for the CPEBs, whereby CPEB1 represses translation during oogenesis and later activates translation in the first meiotic division, CPEB4 activates translation in the second meiotic division (Igea and Mendez 2010). In addition, a specific combination of CPEs mediates the localization of repressed maternal mRNAs to the meiotic spindle, preventing ectopic activation and favoring protein–protein interactions for the chromosomal passenger complex (Eliscovich et al. 2008; Weatheritt et al. 2014). In *Xenopus* oocytes, this mRNA localization is mediated by CPEB1, which colocalizes with microtubules (Groisman et al. 2000; Blower et al. 2007; Brown et al. 2007; Eliscovich et al. 2008). In mitosis, temporal translational regulation is controlled by a variety of mechanisms (Stumpf et al. 2013; Park et al. 2016) including CPEB-mediated changes in poly(A) tail length (Novoa et al. 2010). While CPEB3 is dispensable for mitotic progression, CPEB1, CPEB2 and CPEB4 have sequential and nonredundant function during mitotic progression (Giangarra et al. 2015). However, it is unclear whether regulation of local translation is also required for somatic mitosis, nor which may be the CPEB regulated mRNAs. Here we show that CPEB1 mediates the localization of *CCNB1* and *BUB3* mRNA to the mitotic spindle. Moreover, CPEB1 regulates translation of CCNB1, NEK9, and PLK1, and its depletion leads to aneuploidy. In addition, CPEB4 regulates the synthesis of PRC1 that is critical for spindle midzone formation. Thus, our results demonstrate temporally and spatially restricted translational regulation of spindle-associated mRNAs by CPEB1 and CPEB4.

RESULTS

CPEB1 and translational machinery components are localized at the mitotic spindle

To address if CPEBs could contribute to localization and local translation of CPE-containing mRNAs during mitosis, we first determined if active translation took place associated with mitotic spindles. We observed incorporation of fluorescent AHA, labeling the nascent polypeptide in actively translating ribosomes, associated with the spindle and spindle poles (Fig. 1A). This observation is consistent with the puromycin-labeling of ribosomes at the spindle pole (Blower et al. 2007). Treatment with CDK1 inhibitor RO-3306 was used to reversibly arrest cells at the G2/M phase border. This strategy minimizes the translational perturbation observed when cells are arrested by targeting microtubules (Shuda et al. 2015). Timing after release was adjusted to distinguish between early stages (prophase/metaphase), when CPEB1 is activated by AurKA but not yet degraded by APC in response to CdK1 phosphorylation (Mendez et al. 2000a; Mendez et al. 2002), and late stages (anaphase/telophase), when CPEB1 is degraded and CPEB4 is activated by ERK/CdK1 (Guillén-Boixet et al. 2016). Immunofluorescence on mitotic cells, showed that CPEB1 was distributed along the microtubules and its activatory kinase AurKA (Mendez et al. 2000b), in its active phosphorylated state, was localized at the spindle poles (Fig. 1B). Then, mitotic spindles were purified following the method described by Sillje and Nigg (2006) with modifications to preserve the integrity of associated nucleic acids (see Materials and Methods) (Fig. 1C). Analysis of total cell extract (Tot) and purified spindles (Sp) indicated that CPEB1, components of the CPEB1-mediated translational repression complex (DDX6, PARN, and TACC3) and components of the cytoplasmic polyadenylation and translational activation complex (p-Aurora A, CPSF3, and PABP1) copurified with the spindles; as did TTP and ribosomal protein S6 (Fig. 1D). Small amounts of 4ET and eIF4G were also detected in the spindle fraction. α-tubulin, γ-tubulin, and β-actin were used as positive controls, while GAPDH and TACC2 were negative controls. Thus, both the CPEB1-mediated translational repression and activation complexes are associated with the mitotic spindle.

Then we tested whether CPEB1 depletion had an effect on mitotic progression. Aneuploidy is a potential consequence of impaired mitosis and the defective spindle assembly checkpoint (SAC) (Godek et al. 2015); therefore, we sought to examine the effect of CPEB1 knockdown on genomic stability. To directly assess the ploïdy state, we examined metaphase chromosome spreads of untransfected cells (RPE), a stable RPE cell line expressing a constitutive shRNA against CPEB1 (KD1), or cells expressing a control shRNA (Ctrl); (Supplemental Fig. S1A). CPEB1-deficient cells frequently exhibited an abnormal chromosome number associated with a significant increase in the percentage of aneuploid cells (Fig. 1E). We next investigated whether this phenotype originated from the activity of CPEB1 in the repression of its targets or from their activation after CPEB1 phosphorylation by AurKA. For this, we overexpressed a nonphosphorylable CPEB1 alanine (AA) mutant, a phosphomimetic CPEB1 aspartic (DD) mutant (both in the AurKA targeted residues T172 and S178), or a wild-type CPEB1 (WT); (Supplemental Fig. S1B) and determined their mitotic effects by video microscopy over a 48-h time course (Fig. 1F). Representative still images from the phenotypes observed in the movies are shown in Supplemental Figure S1C. Overall, 82% of the nontransfected cells that entered in mitosis divided correctly into two daughter cells; the remaining 18% either died after entering mitosis, divided in three or more cells, or exited mitosis without dividing. Of the cells with overexpressed WT-CPEB1 that entered mitosis, 67% divided properly, 25% exited mitosis, and 8% either died or divided into three or more cells. In addition, 40% of the cells overexpressing the nonphosphorylable AA-CPEB1 mutant had problems during mitosis: After entering mitosis, only 60% divided properly (i.e., into two daughter cells), 32% did not divide, 7% divided into three or more cells, and 1% died. Similarly, of the phosphomimetic DD-CPEB1-

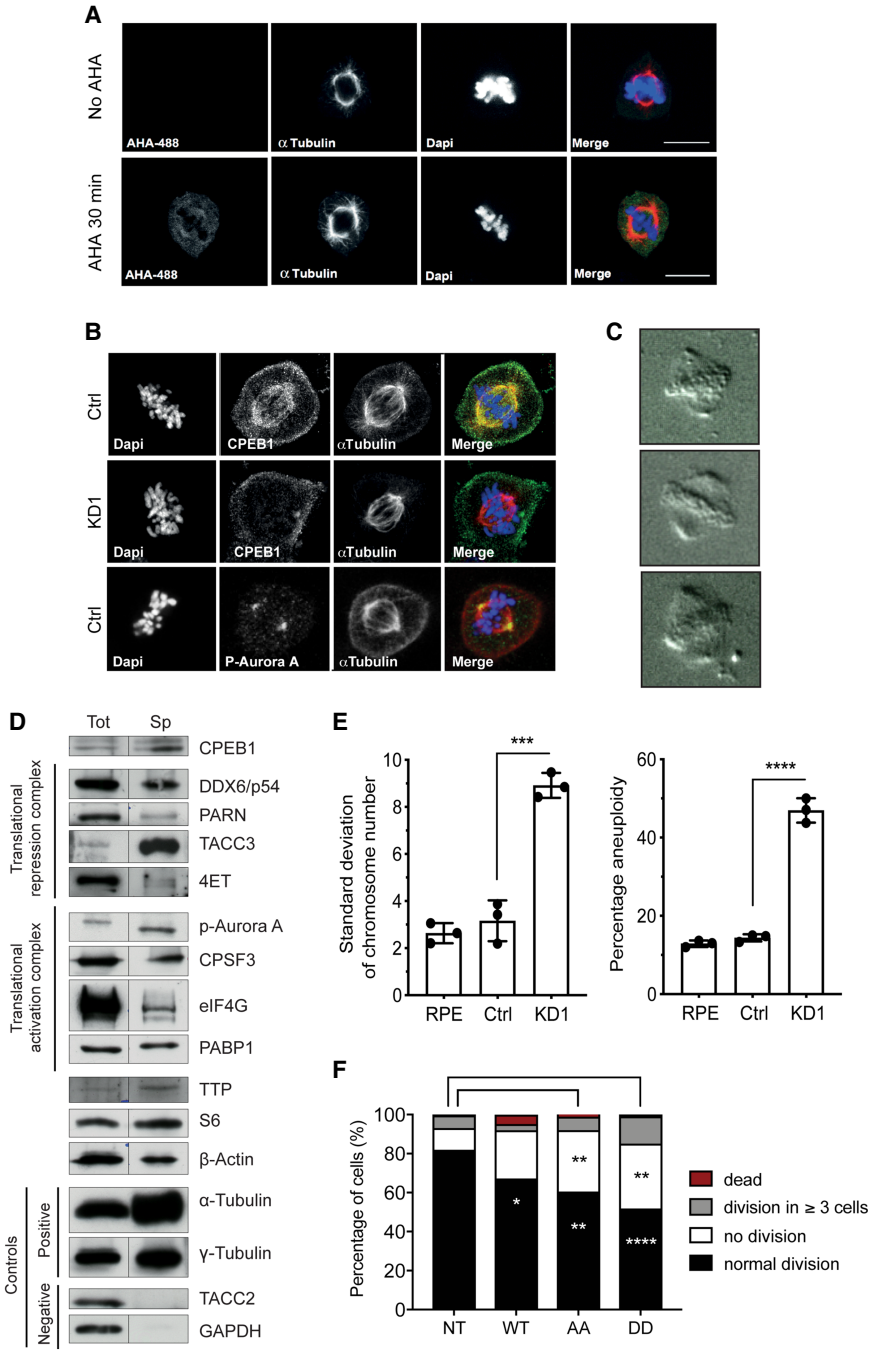

FIGURE 1. CPEB1 and its cofactors are present in the mitotic spindle. (*A*) M-phase synchronized hTERT-RPE1 cells not treated or treated with Click-iT AHA (L-azidohomoalanine). Cells were co-stained with DAPI and α-tubulin antibodies to visualize chromosomes and mitotic spindles, respectively. (*B*) Immunofluorescence images of M-synchronized shCtrl or sh-CPEB1 (KD1) cells, for the indicated proteins and DAPI. (*C*) Representative images of purified mitotic spindles from metaphasic hTERT-RPE1 cells, 45 min after release from the RO-3306 arrest. (*D*) Western blot analysis of total cell extracts (Tot) or purified mitotic spindles (Sp) for the indicated proteins. α-tubulin, γ-tubulin, and β-actin were used as positive controls, and TACC2 and GAPDH were used as negative controls, for spindle localized proteins. Note that for most of the proteins analyzed, two nonadjacent gel lanes were cropped and joined. Equal amounts of protein were loaded in "Tot" and "Sp" lanes. (*E*) Variability in chromosome number (*left*) and percentage of aneuploidy (*right*) in RPE1 wild-type (RPE) or infected with shRNAs control (Ctrl) or against CPEB1 (KD1). Data of three independent experiments are shown here (±SD); between 45 and 70 cells were analyzed in each condition. (*F*) Mitotic outcome (in percentage) classified as cells that normally divided into two daughter cells (Normal division), cells that entered mitosis but could not divide (no division), cells that divided in three or more daughter cells (division in ≥3 cells), and cells that died after entering in mitosis (dead). Conditions correspond to nontransfected cells (NT), cells transfected with wild-type CPEB1 (WT), cells transfected with the nonphosphorylated CPEB1 (AA), or cells transfected with the phosphor-mimetic CPEB1 mutant (DD). Data of three independent experiments are shown here; between 180 and 240 cells were analyzed in each condition. (****) $P < 0.0001$, (**) $P < 0.01$, (*) $P < 0.05$ (two-way ANOVA test).

overexpressing cells that entered mitosis, only 52% divided properly, 33% did not divide, 14% divided into three or more offspring, and 1% died. We concluded that dynamic regulation of CPEB1 phosphorylation is essential for the proper outcome of mitosis, and that its activities in repressing (required for mRNA localization) or activating translation are equally important for cell division.

CPEB1 localizes CPE-containing mRNAs to mitotic spindles

We next asked whether this localization of the CPEB1-complexes at the spindle was linked with mRNA localization. Genome-wide analyses of isolated mRNAs from asynchronous cells, M-phase-arrested cells and purified mitotic spindles showed that 3652 mRNAs were enriched in M-phase over asynchronous, and 3301 mRNAs were enriched in purified spindles over total cellular mRNAs ($\log_2$ ratio > 0.5 and FDR-BH < 1×10^{-5}) (Fig. 2A; Supplemental Table S1). Further, 881 mRNAs were enriched both in M-phase and mitotic spindles, and 2595 (78.6%) of the mRNAs enriched in spindles corresponded to mitotic transcripts, indicating cell cycle specificity. The 881 spindle-associated mRNAs were enriched in CPE-containing transcripts (55.7%, $P = 1.245 \times 10^{-05}$) with the CPE arrangements (Pique et al. 2008), corresponding to both repression (35.55%; $P = 4.252 \times 10^{-06}$) and activation (53.26%; $P = 2.459 \times 10^{-06}$). Interestingly, the *CPEB4* mRNA was one of the CPE-regulated, spindle-associated mRNAs. Indeed, CPEB4 protein copurified also with the spindle (Supplemental Fig. S2A). We validated the spindle association of mRNAs regulated by CPEB1 (e.g., *CCNB1*, *TPX2*, *BUB3*, *CPEB4*, and *ACTB*) by RT-PCR and using GAPDH as a negative control (Fig. 2B). Also, we observed that the depletion of CPEB1 did not affect mRNA levels of *CCNB1* or *BUB3* (Fig. 2C), suggesting that CPEB1 may be involved in regulating their localization or translation.

To confirm the association to the spindle of CPE-containing RNAs in mitotic cells and to determine if this localization was mediated by CPEB1, we selected mRNAs enriched in the purified spindles (*CCNB1* and *BUB3*) and monitored their localization in cells either wild-type (siCTRL) or depleted of CPEB1 (siCPEB1) (Supplemental Fig. S2B). Cells were synchronized in M-phase and analyzed for *CCNB1* and *BUB3* mRNA localization by single molecule fluorescence in situ hybridization (smFISH) (Fig. 2D). In the siCTRL cells, both CPE-regulated mRNAs displayed a punctuated staining pattern, characteristic of mRNPs, which partially colocalized with the spindle. Interestingly, depletion of CPEB1 changed the subcellular localization of *CCNB1* and *BUB3*, which significantly reduced their colocalization with the mitotic spindle, without affecting the total mRNA levels measured by total fluorescence intensity (Fig. 2D–F; Supplemental Fig. S2C). Localization of *GAPDH* mRNA showed a diffuse pattern which did not change upon CPEB1 depletion (Supplemental Fig. S2D). In addition, depletion of CPEB1 also impaired Cyclin B1 synthesis (Fig. 2G), despite the fact that *CCNB1* mRNA levels were unaffected. Taken together, these results indicate that CPE-containing mRNAs associate with the mitotic spindle in a CPEB1-dependent manner and suggests that their proper localization is essential for translation.

Sequential functions of CPEB1 and CPEB4 during mitosis

CPEB1 mediates both translational repression and activation of *CPEB4* mRNA (Igea and Mendez 2010; Calderone et al. 2015). In meiosis, CPEB1 drives early Prometaphase/Metaphase (P/M) activation to be later degraded as the result of Cdk1 phosphorylation. CPEB4 is then synthesized and activated by ERK and Cdk1 to drive translational activation from anaphase, functionally replacing CPEB1 (Mendez et al. 2000a, 2002; Pique et al. 2008; Igea and Mendez 2010; Guillén-Boixet et al. 2016). Because we found both *CPEB4* mRNA and CPEB4 protein at the spindles, we next tested its localization by immunofluorescence. CPEB4 localized in the spindle midzone during late mitosis stages, when CPEB1 is already degraded (Fig. 3A). Next, we tested the mitotic effect of depleting CPEB4. In contrast to CPEB1, CPEB4 depletion did not result in defects in early (P/M) mitosis but only in anaphase. In particular, the time spent in anaphase was reduced as compared with a control siRNA (siCTRL) (Fig. 3B; Supplemental Fig. S2E). This observation is consistent with previously reported results in melanoma cells (Perez-Guijarro et al. 2016) and HEK 293T cells (Giangarra et al. 2015).

To identify CPEB1–4 mRNA targets, we performed RNA immunoprecipitation (RIP)-seq of CPEB1- and CPEB4-bound mRNAs from cells synchronized in G2/M or in early mitotic stages (P/M), respectively (Fig. 3C; Supplemental Fig. S3A; Supplemental Table S1). CPEB4-RIP identified 2849 bound mRNAs and CPEB1-RIP 1870 mRNAs; 616 of these were common for both (Fig. 3C). CPEB1 and CEB4-bound mRNAs were enriched in the spindles as compared with total mRNA (Supplemental Fig. S3B). Overlapping these transcripts with the spindle-associated mRNAs yielded 1372 CPEB4- and 855 CPEB1-targets localized at the spindle, of which 344 were targets of both CPEB1 and CPEB4. Comparison of CPEB1- and CPEB4-target mRNAs (associated or not with the spindle) with their translational efficiency (TE) in G2 versus M (Tanenbaum et al. 2015) showed that the spindle-associated mRNAs behaved differently overall than the cytoplasmic transcripts: While the cytoplasmic CPEB-regulated mRNAs tended to be translationally repressed in M (following the general translation inhibition in M), the spindle-associated mRNAs were often activated in M (Fig. 3D). Gene ontology enrichment showed that spindle-

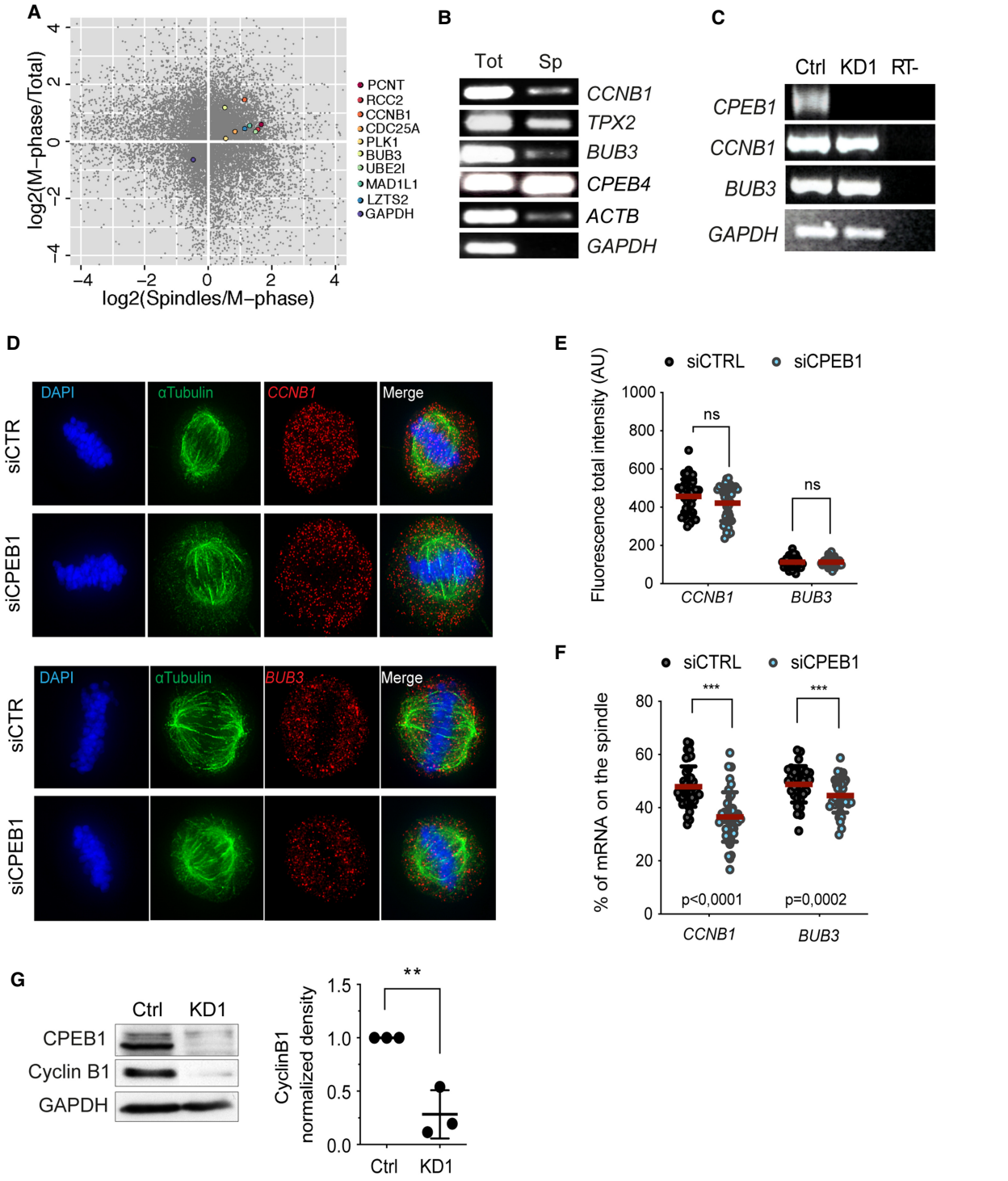

FIGURE 2. CPEB1 regulates localization at the mitotic spindle of CPE-containing mRNAs. (*A*) Genome-wide analysis of spindle-purified mRNAs from HeLa S3 cells, with the scatter plot showing the mRNA enrichment in M phase compared to asynchronous cells (*y* axis), and in spindle-associated transcripts compared to M-phase total transcriptome. (See Supplemental Table 1 for the full list of transcripts). (*B*) RT-PCR of the indicated mRNAs extracted from HeLa S3 cells arrested in P/M (Tot) or from purified mitotic spindles (Sp). GAPDH was used as a negative control. (*C*) RT-PCR of *CPEB1*, *CCNB1*, *BUB3*, and *GAPDH* mRNAs in hTERT-RPE1 control (Ctrl) or CPEB1 sh-RNA (KD1) cells. RT– indicates the control without retrotranscription. (*D*) smFISH images of U2OS cells treated with siRNA control (siCTRL) or siRNA CPEB1 (siCPEB1). Chromosomes and spindles were visualized by DAPI staining and α-tubulin immunofluorescence, respectively. (*E*,*F*) smFISH quantification of U2OS cells treated with siCTRL or siCPEB1. Total fluorescence intensity (*E*) and percentage of the indicated mRNAs localized in the spindles (*F*) in WT and KD1 cells is shown (see Supplemental Fig. S2C for quantification details). (*G*) Representative CPEB1 and Cyclin B1 western blot for WT and KD1 hTERT-RPE1 cells (*left*) and quantification of three independent experiments (*right*).

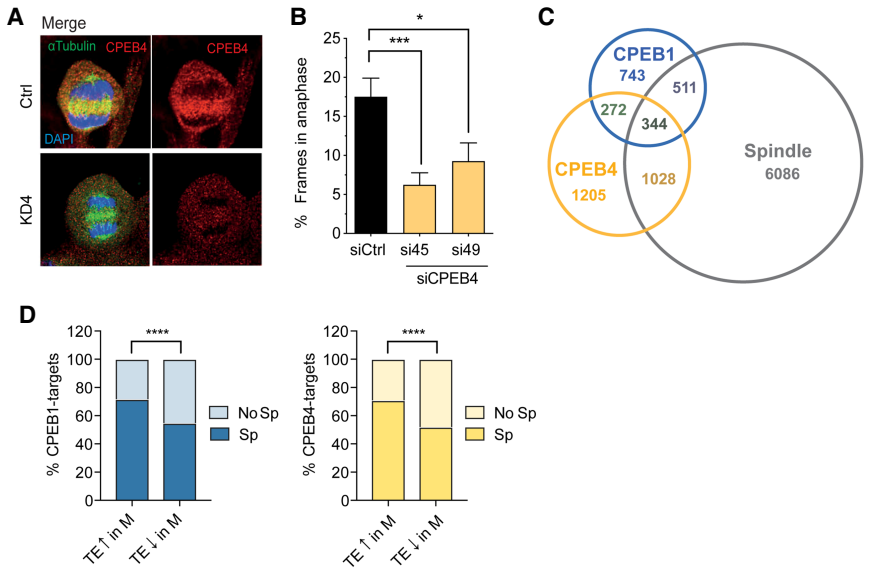

E

	GO-Terms from Top 5 Clusters	GO-Term ID	p_value
CPEB1+CPEB4+Spindle	RNA localization	GO:0006403	8.10E-09
	response to DNA damage stimulus	GO:0006974	4.40E-05
	chromosome organization	GO:0051276	8.00E-05
	intracellular transport	GO:0046907	8.60E-05
	protein ubiquitination	GO:0016567	2.30E-03
CPEB1+CPEB4	cellular protein catabolic process	GO:0030163	5.50E-04
	mRNA processing	GO:0006397	1.20E-03
	phosphate metabolic process	GO:0006796	1.60E-02
	regulation of mRNA stability	GO:0043488	2.60E-02
	protein polyubiquitination	GO:0000209	3.50E-02
CPEB1+Spindle	RNA processing	GO:0006396	6.00E-07
	macromolecular complex assembly	GO:0065003	2.40E-04
	regulation of translation	GO:0006417	4.60E-04
	cell cycle	GO:0007049	1.90E-03
	regulation of cell cycle	GO:0051726	2.50E-03
CPEB4+Spindle	regulation of transcription	GO:0006355	4.70E-07
	cell cycle	GO:0007049	2.20E-06
	response to DNA damage stimulus	GO:0006974	4.20E-05
	vesicle-mediated transport	GO:0016192	6.10E-05
	chromosome organization	GO:0051276	8.70E-04
CPEB1	RNA metabolic process	GO:0016070	3.70E-16
	negative regulation of gene expression	GO:0010629	9.50E-12
	negative regulation of macromolecule metabolic process	GO:0010605	3.90E-11
	positive regulation of macromolecule metabolic process	GO:0010604	3.50E-09
	intracellular transport	GO:0046907	1.50E-07
CPEB4	cellular macromolecular complex assembly	GO:0034622	2.80E-04
	cell division	GO:0051301	6.90E-04
	mitotic cell cycle	GO:0000278	7.40E-04
	peptide metabolic process	GO:0006518	1.40E-03
	DNA repair	GO:0006281	1.20E-02

FIGURE 3. Spindle-localized mRNAs targets of CPEB1 and CPEB4 have sequential cell-cycle related functions. (*A*) Immunofluorescence for CPEB4, α-tubulin, and DAPI in shCtrl (Ctrl) and shCPEB4 (KD4) hTERT-RPE1 cells. (*B*) Quantification of percentage of frames in anaphase from total frames in mitosis for RPE1 cell transfected with a control siRNA (siCtrl) or two siRNAs against CPEB4 (SiCPEB4 #1 and #2). More than 50 cells per condition were quantified. (****) $P < 0.0001$, (**) $P < 0.005$ (Mann–Whitney test). (*C*) Venn diagram showing RIP targets of CPEB1 (*P*-value <0.05), CPEB4 (*P*-value <0.05), and mRNAs localized at the spindle [$\log_2$ (spindle/mitosis) > 0] in Hela S3 cells synchronized with RO3306 (9 µM, 21 h) at the G2/M border and released for 45–60 min for spindle RNA-seq or CPEB4 RIP-seq. (*D*) Percentage of targets from CPEB1 or CPEB4 RIP-seqs localized or not at the spindle that are translationally up-regulated or down-regulated in M versus G2 according to Tanenbaum et al. (2015). (*E*) Top five GO categories of biological processes based on RIP-seq and spindle-seq data analyzed with the functional annotation clustering tool from DAVID bioinformatics resources.

associated and CPEB-bound transcripts were enriched in categories related to cell cycle (including cell cycle/division, chromosome organization, DNA repair and ubiquitination) (Fig. 3E; Supplemental Table S2). More specifically, CPEB1+spindle targets mainly encoded proteins implicated in spindle assembly and checkpoint, whereas CPEB4+spindle targets encoded anaphase and cytokinesis regulators, again suggesting sequential functions for CPEB1 and CPEB4 in the spindle (Supplemental Fig. S3C). In contrast, non-spindle-associated mRNAs were enriched in a wide variety of functions, including RNA processing, stability and cell division (especially for CPEB4) as well as in different metabolic pathways. Naïve discovery of enriched seven-nucleotide motifs (7mers) in CPEB4- and CPEB1-bound 3′UTRs showed that, in addition to previous consensus and nonconsensus CPEs (Pique et al. 2008), "guanine CPE variants" (UUU UUGU, UUUUGUA, and UUUUUUG) were also enriched in CPEB binders (Supplemental Fig. S3D). These new CPE-variants are reminiscent of the binding specificity for the CPEB orthologue Orb2 (Stepien et al. 2016).

Mitotic effectors are regulated by CPEB1 and CPEB4

To test the effects of CPEB1 and CPEB4 on the expression of spindle-associated factors, we selected spindle-localized and CPEB-regulated mRNAs and measured the expression of their encoded proteins in asynchronous (enriched in G1), early M (prophase/metaphase), or late M (anaphase/telophase) cells following CPEBs depletions. NEK9 is a member of the NIMA family kinases activated during prophase at centrosomes and required for mitotic spindle assembly (Bertran et al. 2011). *NEK9* mRNA is bound by both CPEB1 and CPEB4 in M-phase, copurifies with the mitotic spindles (Supplemental Table S1), and its association with ribosomes (ribosome footprints; FPs) is higher in G2/M and M than in G1 (Tanenbaum et al. 2015), suggesting an early activation at the G2/M boundary. Depletion of CPEB1 caused an increase of Nek9 protein levels, but not *NEK9* mRNA, in asynchronous cells (Fig. 4A–C), suggesting that CPEB1 mediates translational repression of *NEK9* mRNA in G1/S phases, at which point AurKA is not active and therefore

CPEB1 is not phosphorylated. However, CPEB1 depletion in P/M, during which AurKA is active and CPEB1 is phosphorylated, blocks Nek9 expression (Fig. 4D,E), suggesting that CPEB1 is a translational activator of *NEK9* mRNA in M-phase. The synthesis of mitotic regulator Polo-like kinase 1 (Plk1) was also found to be dependent on CPEB1 (Fig. 4A–E). Plk1, like CPEB1, is activated by AurA as activating kinase and it is also localized at the mitotic centrosomes (Joukov and De Nicolo 2018). *PLK1* mRNA was bound by CPEB1 and found at the mitotic spindle and, similarly to *NEK9*, it appears to be activated at the G2/M boundary (Supplemental Table S1; Tanenbaum et al. 2015). Upon CPEB1 depletion, Plk1 protein but no mRNA levels show a significant decrease (Fig. 4A–E). The differential behavior of Nek9 and Plk1 protein levels upon CPEB1 depletion in asynchronous cells and during P/M is explained by the CPE combinatorial code (Pique et al. 2008).

We also identified *PRC1* as mRNA bound exclusively by CPEB4, enriched in the spindle-purified fraction and whose association with ribosomes FPs increases in M-phase compared to G1 and G2/M (Tanenbaum et al. 2015), suggesting a late activation during A/T (Supplemental Table S1). PRC1 is a conserved non-motor-crosslinking protein localized in the antiparallel overlaps of microtubules and in the spindle midzone, where it plays an essential role in regulating its formation and cytokinesis (Polak et al. 2016). PRC1 shows a moderate decrease at protein level after CPEB4 depletion, consistent with *PRC1* mRNA being activated by CPEB4 (Fig. 4F–H). Indeed, CPEB4 depletion prevents the normal accumulation of PRC1 in the spindle midzone (Fig. 4I,J).

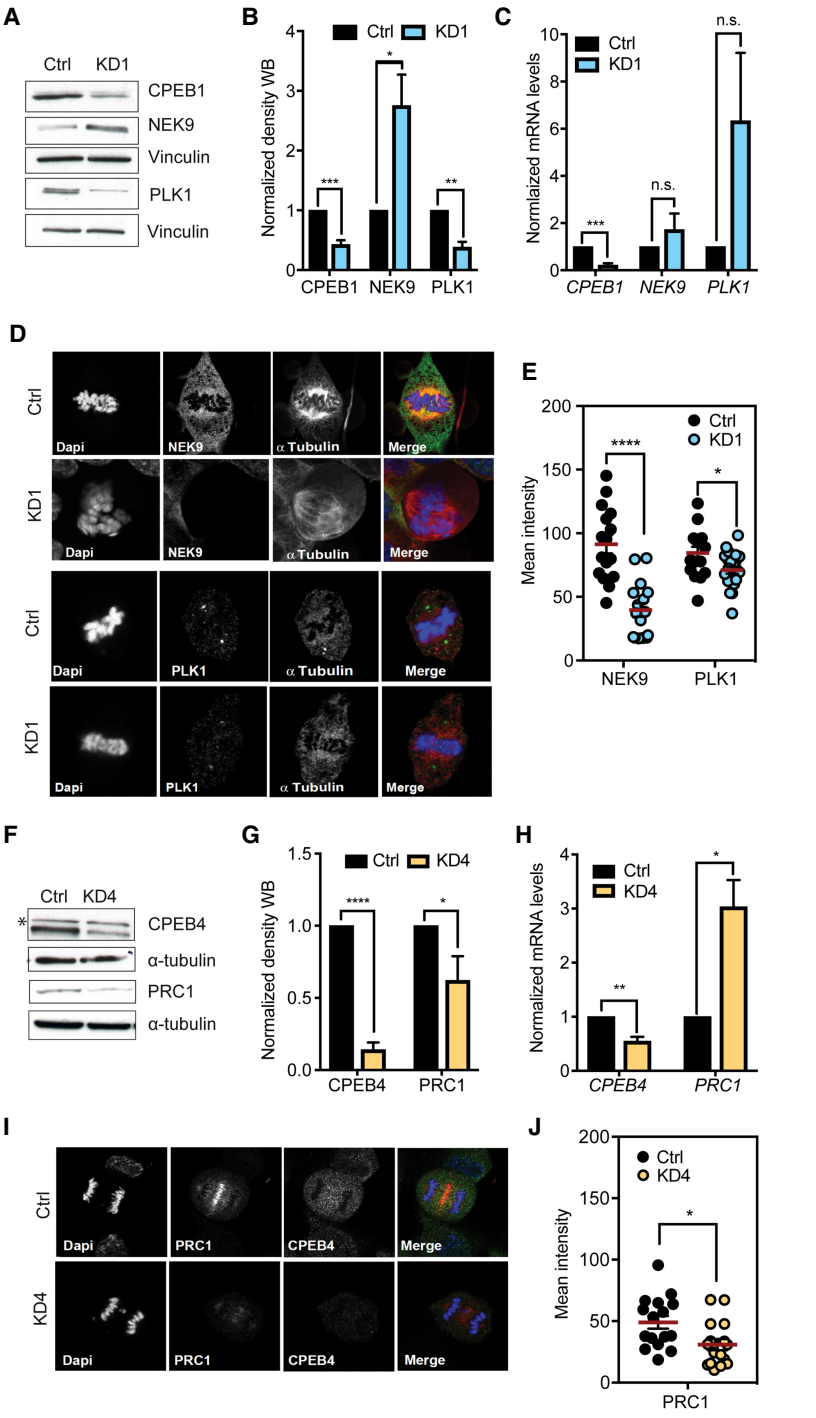

FIGURE 4. CPEB1 and CPEB4 regulate protein expression of mitotic effectors. (*A*) Western blot analysis of Nek9 and PLK1 upon CPEB1 knockdown (KD1) in asynchronous hTERT-RPE1 cells. A representative image is shown, with protein quantification (*B*) and RT-qPCR quantification of mRNA levels in *C*. (*D*) Immunofluorescence of the indicated proteins (Nek9 and PLK1) in Ctrl (ShControl) and KD1 (shCPEB1) hTERT-RPE1 cells synchronized in P/M. Quantification of the immunofluorescence is shown in *E*. (*F*) Western blot analysis of PCR1 upon CPEB4 knockdown (KD4) in asynchronous hTERT-RPE1 cells. A representative image is shown, with protein quantification (*G*) and RT-qPCR quantification of mRNA levels in *H*. (*I*) Immunofluorescence of the PRC1 in Ctrl and KD4 hTERT-RPE1 cells synchronized in A/T after release from the Cdk1 inhibitor. Quantification of the immunofluorescence is shown in *J*. Results from three independent experiments. Statistics of immunofluorescence images by Mann–Whitney test (****) $P < 0.0001$, (**) $P < 0.005$.

DISCUSSION

Although in mitosis cap-dependent translation is reduced (Stumpf et al. 2013; Kim et al. 2014; Aviner et al. 2015; Tanenbaum et al. 2015; Park

et al. 2016), a relatively modest number of mRNAs, such as IRES- or CPE-containing transcripts, are activated to sustain accurate chromosome segregation and cell survival during mitosis (Pyronnet et al. 2000; Qin and Sarnow 2004; Barna et al. 2008; Novoa et al. 2010). In mitosis, temporal translational regulation is controlled by a variety of mechanisms (Stumpf et al. 2013; Park et al. 2016) including CPEB-mediated changes in poly(A) tail length (Novoa et al. 2010; Giangarra et al. 2015). In *Xenopus* oocytes, this temporal regulation is coupled to mRNA localization of repressed mRNAs and local activation of translation. This localized translation is, at least in part, mediated by CPEs and CPEB1 directing the localization of repressed maternal mRNAs to the meiotic spindle, preventing ectopic activation and favoring protein–protein interactions for the chromosomal passenger complex (Groisman et al. 2000; Blower et al. 2007; Brown et al. 2007; Eliscovich et al. 2008).The need for localized translation in oocytes probably arises from its large size, with a volume of 1 µl and a spindle size similar to a mitotic somatic cell (Mitchison et al. 2015). However, it remained unclear whether such regulation of local translation is also required for somatic mitosis.

Here we show that CPEB1 and CPEB4 localize, together with components of their mRNPs and CPE-containing mRNAs, at the mitotic spindle. Indeed, we can visualize translation at the mitotic spindle and, at least for CCNB1, we show that its mRNA localization and synthesis require CPEB1. Moreover, CPEB1 and CPEB4 appear to have sequential functions in mitosis corresponding with the described roles of factors encoded by their spindle-associated target transcripts. Accordingly, Gene Ontology terms for mitotic spindle-associated RNAs bound by CPEB1 and CPEB4 are enriched in categories related to RNA localization, DNA repair and chromosome organization. Particularly, CPEB1 was found to bind transcripts relevant for early stages of mitosis, whereas CPEB4 targets encoded late mitotic effectors, again suggesting sequential functions for CPEB1 and CPEB4 in the spindle (Supplemental Fig. S3C). Altogether, our results suggest a key role of CPEB1 and CPEB4 in mitotic spindle localized translational regulation consistent with the following model (Supplemental Fig. S4).

Prior to P/M transition, unphosphorylated CPEB1 would mediate translational repression and localization of a subset of mRNAs. During prophase/prometaphase, these repressor CPEB1 mRNPs would localize in the perichromosomal region and along the spindle until they reach the spindle pole. At the spindle, p-AurKA activates CPEB1, which in turn would trigger local translation of CPE-regulated mRNAs at the spindle poles. Among these CPEB1-localized mRNAs are *CCNB1* and *BUB3*. CPEB4 then accumulates in the spindle midzone (interpolar microtubules) between the migrating chromatids. During metaphase/anaphase, CyclinB1/CdK1 and Plk1 promote the degradation of CPEB1 (Mendez et al. 2002; Setoyama et al. 2007). Concomitantly, ERK and Cdk1 activate CPEB4 (Guillén-Boixet et al. 2016), thus promoting the replacement of CPEB1 by CPEB4 to sustain sequential activation of CPE-regulated mRNAs in the spindle. CPEB4 regulation is driven by intrinsically disordered regions that are also present in other spindle-associated components (Jiang et al. 2015). Indeed, coacervation of proteins has been suggested as a mechanism by which the spindle matrix promotes spindle assembly by concentrating its building blocks (in this case, proteins and mRNAs) in a membraneless organelle. In the last steps of mitosis, activated CPEB4 at the spindle midzone would promote translation of mRNAs encoding anaphase or cytokinesis factors, such as PRC1. A sequential order might be coordinated at two levels: first, by the local translation of *CPEB4* mRNA, and second, by the posttranslational regulation of CPEB1 and CPEB4 by Cdk1, which inactivates CPEB1 and activates CPEB4 in anaphase.

MATERIALS AND METHODS

Cell culture, transfections, and knockdown

hTERT-RPE1 cells were grown in Ham-F12 media with 10% FBS, and HeLa S3 cells and HEK 293T cells, in DMEM with 10% FBS. Cells were transfected with Effectene following the manufacturer's instructions. A CPEB1-inducible knockdown RPE1 cell line was generated as previously described (Calderone et al. 2015), with the following modifications: hTERT-RPE1 cells were transduced with pLKO IPTG Lac0 lentivector carrying a sequence for CPEB1 shRNAs expression (5′-AGGCGTTCCTTGGGATATTAC-3′, Sigma). Virus production was performed as indicated in http ://tronolab.epfl.ch/. CPEB1-inducible knockdown RPE1 cells were cultured for 4 d in DMEM supplemented with 10% FBS, 2 mM L-glutamine and 1% penicillin/streptomycin, in the presence of PBS for the control (1 µL ml^{-1} of medium) or IPTG (5 µM isopropyl-β-D-thio-galactoside) in order to induce the expression of the shRNA directed against CPEB1. Transient knockdown was obtained with shRNA human CPEB1 TRCN0000149456 and shRNA human CPEB4 TRCN0000156565 cloned in the pLKO.1. Mission siRNAs against CPEB4 were used when indicated. siRNA transfection in U2OS was performed using Lipofectamine RNAiMax (Thermo Fisher Scientific) according to manufacturer's instructions at 50 nM for 48 h. Predesigned SMARTpool siRNAs were obtained from Dharmacon.

Immunofluorescence

Cells were grown on glass coverslips, synchronized in P/M by adding RO3306 during 21 h at 9 µM followed by a release of 35–45 min, washed with PBS and fixed either with cold methanol for 10 min or with 4% paraformaldehyde for 20 min at room temperature. Cells were permeabilized in 0.1% Triton X-100 for 10 min and saturated for 30 min with 0.2% BSA. Cells were then incubated 1 h at room temperature with primary antibodies, washed in PBS, stained with the secondary antibodies, and then mounted

in DAPI containing Vectashield (Vector Laboratories). Images were obtained on an inverted Leica TCS SP5 confocal microscopy.

Immunoblotting

Protein extracts were quantified by DC Protein assay (Bio-Rad), and equal amounts of proteins were separated by SDS–polyacrylamide gel electrophoresis. After transfer of proteins onto a nitrocellulose membrane (GE10600001, Sigma) for 1 h at 400 mA, membranes were blocked for 1 h in 5% milk, and specific proteins were labeled with the mentioned antibodies.

Plasmids and antibodies

The following antibodies were used from Abcam: anti-Phospho CPEB1 S174 (ab10890) (Calderone et al. 2015), anti-CPEB4, anti-TACC3 (ab56595), TACC2 (ab17916), anti-Aurora-A (ab13824), DDX6 (ab40684), anti-Nek9, and anti-PRC1; from Sigma: anti-PARN (HPA006314), anti-α-tubulin and anti-γ-tubulin; from Santa Cruz Biotechnology: anti-CPEB1 (H-300), anti-CPSF1 (B-5; sc-166282), anti-CPSF3 (ww-2; sc-100691), TTP (sc-8458), anti-eIF4E (c-20), and anti-GAPDH (sc32233); from Cell Signaling: anti-phospho-Aurora A (Thr288; 2914), anti-4ET (2297), anti-PABP (4992), anti-S6 (2317), anti-eIF4G (2498), and anti-CPEB1 (13583); and anti-CPEB1 (Proteintech).

Spindle purification

Mitotic spindles were purified as previously described (Sillje and Nigg 2006) with some modifications. Briefly, Hela S3 cells were first synchronized with thymidine for 16 h and then synchronized at the G2/M border with 9 μM RO3306 for 21 h. After release (35–45 min), mitotic cells were collected by mitotic shake-off and treated as described (Sillje and Nigg 2006) but without adding RNases to the lysis buffer.

smFISH in combination with immunofluorescence

U2OS cells were grown on the coverslips and synchronized with 7.5 μM RO-3306 for 18 h, followed by 35 min release. For the smFISH, the samples were prepared as previously described with minor modifications (Raj and Tyagi 2010). Briefly, samples were fixed for 10 min with 4% Formaldehyde solution (Sigma-Aldrich) and permeabilized with 0.01% Triton X-100 for 10 min. Afterwards, samples were subjected to immunofluorescence staining (α-tubulin, 4°C overnight). Samples were then fixed for 10 min with 4% Formaldehyde solution (Sigma-Aldrich) and hybridized with smFISH probes (Stellaris, Biosearch Technologies) for 4 h at 37°C. Coverslips were mounted to the microscopy slide using Prolong Diamond Antifade (Invitrogen). The images were acquired on a deconvolution system (DeltaVision RT; Applied Precision) using a 60× lens. Experiments were performed with custom made smFISH probes designed by Stellaris (Biosearch Technologies). All probes were labeled with a Quasar 670 fluorophore and designed by using Probe Designer Tool (http://www.biosearchtech.com/stellarisdesigner/). The quantification of spindle-localized mRNA particles was performed by taking two distinct regions of interest (ROI) per cell: (i) ROI1 covered mitotic spindle area (as assessed by αTubulin staining) and (ii) ROI2 covered region between the mitotic spindle and cell border. The total mRNA number was determined as a sum of both ROIs. The number of spindle-associated mRNAs was calculated by dividing the number of mRNAs measured in ROI1 over total mRNA number in each individual cell.

Metaphase spreads

Cells were grown in 35-mm dishes, with fresh media added 3 h before harvesting. KaryoMax Colcemid Solution (Gibco BRL) was then added and left for 2 h at 37°C. Cells were centrifuged and resuspended in 0.56% KCl for 30 min at 37°C and then fixed with a 3:1 methanol:acetic acid solution. The resulting nuclei suspension was dropped onto slides and air-dried before adding Vectashield with DAPI. Diploidy (46 chromosomes) or aneuploidy (more or less than 46 chromosomes) was determined for each sample by counting metaphase chromosomes.

RNA-immunoprecipitation sequencing (RIP) analysis

Hela S3 cells were cultured in DMEM supplemented with 10% FBS and incubated with RO-3306 (21 h, 9 μM) (followed by a 1-h release for anti-CPEB4 RIP). Cells were rinsed twice with 10 mL PBS and incubated with PBS and 0.5% formaldehyde for 5 min at room temperature under constant soft agitation to cross-link RNA-binding proteins to target RNAs. Crosslinking reactions were quenched by adding a final concentration of 0.25 M glycine for 5 min. Cells were washed twice with 10 mL PBS, lysed with a scraper and RIPA buffer (25 mM Tris-Cl pH 7.6, 1% Nonidet P-40, 1% sodium deoxycholate, 0.1% SDS, 100 mM EDTA, 150 mM NaCl, protease inhibitor cocktail, RNase inhibitors), and sonicated for 10 min at low intensity with a Standard Bioruptor Diagenode. After centrifugation (10 min, max speed, 4°C), supernatants were collected, precleared and immunoprecipitated (4 h, 4°C, on rotation) with 10 μg of anti-CPEB4 antibody, anti-CPEB1 (Proteintech) or rabbit IgG (Sigma) bound to 50 mL of Dynabeads Protein A (Invitrogen). Beads were washed four times with cold RIPA buffer supplemented with protease inhibitors, resuspended in 100 mL proteinase K buffer with 70 mg of proteinase K (Roche) and incubated for 60 min at 65°C. RNA was extracted by standard phenol–chloroform. Samples were processed at the IRB Functional Genomics Facility following standard procedures. Illumina 100 bp single-end RIP-Seq data were aligned against *Homo sapiens* hg19 reference genome using Bowtie2 v2.2.2 (Langmead and Salzberg 2012) in local mode, allowing one mismatch in the read seed (–local –N 1). Duplicated reads potentially arising from amplification artefacts were detected and removed with sambamba v0.5.1 (Tarasov et al. 2015) using default options. Afterwards, significantly enriched regions between IP against input samples were detected using the enrichedRegions function of the htSeqTools package (Planet et al. 2012) with default settings and a Benjamini–Hochberg adjusted *P*-value lower than 0.05. Gene ontology enrichment analysis was performed using the DAVID Bioinformatics Resources Functional Annotation Tool (http://david.abcc.ncifcrf.gov, Huang et al. 2007). Data was deposited at NCBI GEO repository (accession number GSE99810/password: odczomgirlqvnub).

Video microscopy

For live imaging analysis, Histone H2B transfected cells were seeded in a 24-well imaging plate (zell-kontakt) in a humidified 5% CO_2 atmosphere at 37°C on a temperature-controlled spinning disk microscope (Andor). Images were captured every 10 min for 15 h. Cells were analyzed by an automated inverted microscope (TIRF, ScanR Olympus), and images were processed using ImageJ software.

mRNA library generation and sequencing

Illumina bclConverter script from Offline BaseCaller (OLB) version 1.9 was used to convert individual lane/tile/cycle binary basecalling files (.bcl) to ASCII FASTQ format. Illumina GERALD software from CASAVA 1.7.0 was used to generate final per-lane FASTQ sequence files.

mRNAseq analysis

Five fastq files were generated containing the sequencing data for each of the four mRNAseq libraries. The quality and number of the reads for each sample were then assessed using FASTQC v0.9.3 (http://www.bioinformatics.bbsrc.ac.uk/projects/fastqc/), and adapter contamination was removed from the original reads using the cutadapt v0.9.4 software (http://code.google.com/p/cutadapt/). Reads shorter than 25 bp after adapter trimming and quality filtering were discarded. Reads that passed the quality-control steps were then aligned to Ensembl (v63) annotated human transcripts using Bowtie v0.12.5, allowing two mismatches (–best -v 2 -a) (Langmead 2010). Assessing read-coverage along the transcripts, we detected that samples from spindles fall in coverage toward the 5′ end, reaching the levels of synchronized samples 500 nt from the 3′ end. This was taken into account when calculating the relative differences, as described below.

Differential mRNA abundance analysis

Reads over the 500 nt at the 3′ end of transcripts were used to generate read-count tables for all samples. Only genes that had at least an average of 10 read counts were analyzed for evidence of differential abundance. Counts were normalized across samples using full-quantile normalization with the EDA package (Risso et al. 2011). Identification of statistically significant differences in the abundance of mRNAs was performed with DEseq (Anders and Huber 2010), comparing M-phase synchronized with total mRNA samples, and spindles associated with M-phase synchronized samples. Transcripts were defined as having a significant different abundance for a $\log_2$-fold change >0.5 and a Benjamini and Hochberg corrected FDR $<1 \times 10^{-5}$. The intersection of genes identified in both comparisons were used to select the set of spindle-associated mRNA candidates.

3′-UTR properties sequence analysis

Transcripts with available 3′-UTR sequences were scanned for the presence of CPE related *k*-mers: the hexanucleotide motif (Hex), the cytoplasmic polyadenylation elements (CPE), Pumilio-binding elements (PBE), and AU-rich elements (ARE). The presence and relative distances of these motifs defined the putative regulation according to the model defined previously (Pique et al. 2008). In order to evaluate the overrepresentation of each kind of regulatory arrangement, the proportions of spindle-associated mRNAs were compared against the set of all mRNAs expressed in any condition with Fisher's exact test. Enrichment assessment of all possible 7-mers was performed on CPEB4 and CPEB1 bound 3′UTRs as described (Agirre et al. 2015).

Statistics and reproducibility

Data are expressed as mean ± standard error of the mean (S.E.M.) unless otherwise specified. Immunofluorescence images are always representative of three independent experiments. Data set statistics were analyzed using the GraphPad Prism software. Statistics by two-tailed unpaired *t*-test unless otherwise stated. Significant differences: * $P < 0.05$, ** $P < 0.01$, *** $P < 0.001$.

SUPPLEMENTAL MATERIAL

Supplemental material is available for this article.

ACKNOWLEDGMENTS

We thank the Advance Digital Microscopy, Biostatistics/Bioinformatics, and Functional Genomics facilities at IRB Barcelona. We also thank members of Dr. Méndez's laboratory for useful discussions. This work was supported by grants from the Spanish Ministry of Economy and Competitiveness (MINECO, BFU2014-54122-P, Consolider RNAREG CSD2009-00080), the European Union FEDER funds, the Fundación Botín by the Banco Santander through its Santander Universities Global Division, the Scientific Foundation of the Spanish Association Against Cancer (AECC), and the Worldwide Cancer Research Foundation. R.P. held a "la Caixa" predoctoral fellowship. IRB Barcelona is the recipient of a Severo Ochoa Award of Excellence from MINECO (Government of Spain).

Author contributions: R.P. performed and contributed to the design, data analysis and interpretation of experiments. R.P. and A.M-R. contributed to manuscript and figure preparation. C.S-M. performed experiments and contributed to data analysis. M.O. performed the smFISH experiments. N.B. performed the bioinformatics analyses for spindle-associated RNAs. E.B. and C.L.C. performed knock-down experiments. O.R. performed the bioinformatic analysis for RIP-seq experiments. E.E. supervised bioinformatic analysis. R.M. conceived, directed, and discussed the study and wrote the manuscript with contributions of M.M.M.

Received August 12, 2020; accepted December 2, 2020.

REFERENCES

Agirre E, Bellora N, Alló M, Pages A, Bertucci P, Kornblihtt AR, Eyras E. 2015. A chromatin code for alternative splicing involving a putative association between CTCF and HP1α proteins. *BMC Biol* **13:** 31. doi:10.1186/s12915-015-0141-5

Anders S, Huber W. 2010. Differential expression analysis for sequence count data. *Genome Biol* **11:** R106. doi:10.1186/gb-2010-11-10-r106

Aviner R, Shenoy A, Elroy-Stein O, Geiger T. 2015. Uncovering hidden layers of cell cycle regulation through integrative multi-omic analysis. *PLoS Genet* **11:** e1005554. doi:10.1371/journal.pgen.1005554

Barna M, Pusic A, Zollo O, Costa M, Kondrashov N, Rego E, Rao PH, Ruggero D. 2008. Suppression of Myc oncogenic activity by ribosomal protein haploinsufficiency. *Nature* **456:** 971–975. doi:10.1038/nature07449

Belloc E, Mendez R. 2008. A deadenylation negative feedback mechanism governs meiotic metaphase arrest. *Nature* **452:** 1017–1021. doi:10.1038/nature06809

Bertran MT, Sdelci S, Regue L, Avruch J, Caelles C, Roig J. 2011. Nek9 is a Plk1-activated kinase that controls early centrosome separation through Nek6/7 and Eg5. *EMBO J* **30:** 2634–2647. doi:10.1038/emboj.2011.179

Blower MD, Feric E, Weis K, Heald R. 2007. Genome-wide analysis demonstrates conserved localization of messenger RNAs to mitotic microtubules. *J Cell Biol* **179:** 1365–1373. doi:10.1083/jcb.200705163

Brown KS, Blower MD, Maresca TJ, Grammer TC, Harland RM, Heald R. 2007. Xenopus tropicalis egg extracts provide insight into scaling of the mitotic spindle. *J Cell Biol* **176:** 765–770. doi:10.1083/jcb.200610043

Calderone V, Gallego J, Fernandez-Miranda G, Garcia-Pras E, Maillo C, Berzigotti A, Mejias M, Bava FA, Angulo-Urarte A, Graupera M, et al. 2015. Sequential functions of CPEB1 and CPEB4 regulate pathologic expression of VEGF and angiogenesis in chronic liver disease. *Gastroenterology* **150:** 982–997.e30. doi:10.1053/j.gastro.2015.11.038

Eliscovich C, Peset I, Vernos I, Mendez R. 2008. Spindle-localized CPE-mediated translation controls meiotic chromosome segregation. *Nat Cell Biol* **10:** 858–865. doi:10.1038/ncb1746

Giangarra V, Igea A, Castellazzi CL, Bava FA, Mendez R. 2015. Global analysis of CPEBs reveals sequential and non-redundant functions in mitotic cell cycle. *PLoS ONE* **10:** e0138794. doi:10.1371/journal.pone.0138794

Godek KM, Kabeche L, Compton DA. 2015. Regulation of kinetochore-microtubule attachments through homeostatic control during mitosis. *Nat Rev Mol Cell Biol* **16:** 57–64. doi:10.1038/nrm3916

Groisman I, Huang YS, Mendez R, Cao Q, Theurkauf W, Richter JD. 2000. CPEB, maskin, and cyclin B1 mRNA at the mitotic apparatus: implications for local translational control of cell division. *Cell* **103:** 435–447. doi:10.1016/S0092-8674(00)00135-5

Guillén-Boixet JB V, Salvatella X, Méndez R. 2016. CPEB4 is regulated during cell cycle by ERK2/Cdk1-mediated phosphorylation and its assembly into liquid-like droplets. *Elife* **5:** e19298. doi:10.7554/eLife.19298

Huang DW, Sherman BT, Tan Q, Kir J, Liu D, Bryant D, Guo Y, Stephens R, Baseler MW, Lane HC, et al. 2007. DAVID Bioinformatics Resources: expanded annotation database and novel algorithms to better extract biology from large gene lists. *Nucleic Acids Res* **35:** W169–W175. doi:10.1093/nar/gkm415

Igea A, Mendez R. 2010. Meiosis requires a translational positive loop where CPEB1 ensures its replacement by CPEB4. *EMBO J* **29:** 2182–2193. doi:10.1038/emboj.2010.111

Jiang H, Wang S, Huang Y, He X, Cui H, Zhu X, Zheng Y. 2015. Phase transition of spindle-associated protein regulate spindle apparatus assembly. *Cell* **163:** 108–122. doi:10.1016/j.cell.2015.08.010

Joukov V, De Nicolo A. 2018. Aurora-PLK1 cascades as key signaling modules in the regulation of mitosis. *Sci Signal* **11:** eaar4195. doi:10.1126/scisignal.aar4195

Kim Y, Lee JH, Park JE, Cho J, Yi H, Kim VN. 2014. PKR is activated by cellular dsRNAs during mitosis and acts as a mitotic regulator. *Genes Dev* **28:** 1310–1322. doi:10.1101/gad.242644.114

Langmead B. 2010. Aligning short sequencing reads with Bowtie. *Curr Protoc Bioinformatics* **Chapter 11:** Unit 11 17. doi:10.1002/0471250953.bi1107s32

Langmead B, Salzberg SL. 2012. Fast gapped-read alignment with Bowtie 2. *Nat Methods* **9:** 357–359. doi:10.1038/nmeth.1923

Mendez R, Hake LE, Andresson T, Littlepage LE, Ruderman JV, Richter JD. 2000a. Phosphorylation of CPE binding factor by Eg2 regulates translation of c-mos mRNA. *Nature* **404:** 302–307. doi:10.1038/35005126

Mendez R, Murthy KG, Ryan K, Manley JL, Richter JD. 2000b. Phosphorylation of CPEB by Eg2 mediates the recruitment of CPSF into an active cytoplasmic polyadenylation complex. *Mol Cell* **6:** 1253–1259. doi:10.1016/S1097-2765(00)00121-0

Mendez R, Barnard D, Richter JD. 2002. Differential mRNA translation and meiotic progression require Cdc2-mediated CPEB destruction. *EMBO J* **21:** 1833–1844. doi:10.1093/emboj/21.7.1833

Mitchison TJ, Ishihara K, Nguyen P, Wuhr M. 2015. Size scaling of microtubule assemblies in early *Xenopus* embryos. *Cold Spring Harb Perspect Biol* **7:** a019182. doi:10.1101/cshperspect.a019182

Novoa I, Gallego J, Ferreira PG, Mendez R. 2010. Mitotic cell-cycle progression is regulated by CPEB1 and CPEB4-dependent translational control. *Nat Cell Biol* **12:** 447–456. doi:10.1038/ncb2046

Park JE, Yi H, Kim Y, Chang H, Kim VN. 2016. Regulation of poly(A) tail and translation during the somatic cell cycle. *Mol Cell* **62:** 462–471. doi:10.1016/j.molcel.2016.04.007

Perez-Guijarro E, Karras P, Cifdaloz M, Martinez-Herranz R, Canon E, Grana O, Horcajada-Reales C, Alonso-Curbelo D, Calvo TG, Gomez-Lopez G, et al. 2016. Lineage-specific roles of the cytoplasmic polyadenylation factor CPEB4 in the regulation of melanoma drivers. *Nat Commun* **7:** 13418. doi:10.1038/ncomms13418

Pique M, Lopez JM, Foissac S, Guigo R, Mendez R. 2008. A combinatorial code for CPE-mediated translational control. *Cell* **132:** 434–448. doi:10.1016/j.cell.2007.12.038

Planet E, Attolini CS, Reina O, Flores O, Rossell D. 2012. htSeqTools: high-throughput sequencing quality control, processing and visualization in R. *Bioinformatics* **28:** 589–590. doi:10.1093/bioinformatics/btr700

Polak B, Risteski P, Lesjak S, Tolic IM. 2016. PRC1-labeled microtubule bundles and kinetochore pairs show one-to-one association in metaphase. *EMBO Rep* **18:** 217–230. doi:10.15252/embr.201642650

Pyronnet S, Pradayrol L, Sonenberg N. 2000. A cell cycle-dependent internal ribosome entry site. *Mol Cell* **5:** 607–616. doi:10.1016/S1097-2765(00)80240-3

Qin X, Sarnow P. 2004. Preferential translation of internal ribosome entry site-containing mRNAs during the mitotic cycle in mammalian cells. *J Biol Chem* **279:** 13721–13728. doi:10.1074/jbc.M312854200

Raj A, Tyagi S. 2010. Detection of individual endogenous RNA transcripts in situ using multiple singly labeled probes. *Methods Enzymol* **472:** 365–386. doi:10.1016/S0076-6879(10)72004-8

Richter JD. 2007. CPEB: a life in translation. *Trends Biochem Sci* **32:** 279–285. doi:10.1016/j.tibs.2007.04.004

Risso D, Schwartz K, Sherlock G, Dudoit S. 2011. GC-content normalization for RNA-seq data. *BMC Bioinformatics* **12:** 480. doi:10.1186/1471-2105-12-480

Setoyama D, Yamashita M, Sagata N. 2007. Mechanism of degradation of CPEB during *Xenopus* oocyte maturation. *Proc Natl Acad Sci* **104:** 18001–18006. doi:10.1073/pnas.0706952104

Shuda M, Velasquez C, Cheng E, Cordek DG, Kwun HJ, Chang Y, Moore PS. 2015. CDK1 substitutes for mTOR kinase to activate mitotic cap-dependent protein translation. *Proc Natl Acad Sci* **112:** 5875–5882. doi:10.1073/pnas.1505787112

Sillje HH, Nigg EA. 2006. Purification of mitotic spindles from cultured human cells. *Methods* **38:** 25–28. doi:10.1016/j.ymeth.2005.07.006

Stepien BK, Oppitz C, Gerlach D, Dag U, Novatchkova M, Kruttner S, Stark A, Keleman K. 2016. RNA-binding profiles of *Drosophila* CPEB proteins Orb and Orb2. *Proc Natl Acad Sci* **113:** E7030–E7038. doi:10.1073/pnas.1603715113

Stumpf CR, Moreno MV, Olshen AB, Taylor BS, Ruggero D. 2013. The translational landscape of the mammalian cell cycle. *Mol Cell* **52:** 574–582. doi:10.1016/j.molcel.2013.09.018

Tanenbaum ME, Stern-Ginossar N, Weissman JS, Vale RD. 2015. Regulation of mRNA translation during mitosis. *Elife* **4:** e07957. doi:10.7554/eLife.07957

Tarasov A, Vilella AJ, Cuppen E, Nijman IJ, Prins P. 2015. Sambamba: fast processing of NGS alignment formats. *Bioinformatics* **31:** 2032–e02034. doi:10.1093/bioinformatics/btv098

Weatheritt RJ, Gibson TJ, Babu MM. 2014. Asymmetric mRNA localization contributes to fidelity and sensitivity of spatially localized systems. *Nat Struct Mol Biol* **21:** 833–839. doi:10.1038/nsmb.2876

Weill L, Belloc E, Bava FA, Mendez R. 2012. Translational control by changes in poly(A) tail length: recycling mRNAs. *Nat Struct Mol Biol* **19:** 577–585. doi:10.1038/nsmb.2311

mRNA spindle localization and mitotic translational regulation by CPEB1 and CPEB4

Rosa Pascual, Carolina Segura-Morales, Manja Omerzu, et al.

RNA 2021 27: 291-302 originally published online December 15, 2020
Access the most recent version at doi:10.1261/rna.077552.120